Reference: *Biol. Bull.* **201:** 136–153. (October 2001)

Ontogenetic Changes in Fibrous Connective Tissue Organization in the Oval Squid, *Sepioteuthis lessoniana* Lesson, 1830

JOSEPH T. THOMPSON* AND WILLIAM M. KIER

Department of Biology, CB#3280 Coker Hall, University of North Carolina, Chapel Hill, North Carolina 27599-3280

Abstract. Ontogenetic changes in the organization and volume fraction of collagenous connective tissues were examined in the mantle of *Sepioteuthis lessoniana*, the oval squid. Outer tunic fiber angle (the angle of a tunic collagen fiber relative to the long axis of the squid) decreased from 33.5° in newly hatched animals to 17.7° in the largest animals studied. The arrangement of intramuscular collagen fiber systems 1 (IM-1) and 2 (IM-2) also changed significantly during ontogeny. Because of the oblique trajectory of the IM-1 collagen fibers, two fiber angles were needed to describe their organization: (1) IM-1_{SAG}, the angle of an IM-1 collagen fiber relative to the squid's long axis when viewed from a sagittal plane and (2) IM-1_{TAN}, the angle of an IM-1 collagen fiber relative to the squid's long axis when viewed from a plane tangential to the outer curvature of the mantle. The sagittal component (IM-1_{SAG}) of the IM-1 collagen fiber angle was lowest in hatchling squid (32.7°) and increased exponentially during growth to 43° in squid with a dorsal mantle length (DML) of 15 mm. In squid larger than 15 mm DML, IM-1_{SAG} fiber angle did not change. The tangential component (IM-1_{TAN}) of IM-1 collagen fiber angle was highest in hatchling squid (39°) and decreased to 32° in the largest squid examined. IM-2 collagen fiber angle (the angle of an IM-2 collagen fiber relative to the outer surface of the mantle) was lowest in hatchling squid (34.6°) and increased exponentially to about 50° in 15-mm DML animals. In squid larger than 15 mm DML, IM-2 fiber angle increased slightly with size. The volume fraction of collagen in IM-1 and IM-2 increased 68 and 36 times, respectively, during growth. The ontogenetic changes in the organization of collagen fibers in the outer tunic, IM-1, and IM-2 may lead to ontogenetic differences in the kinematics of mantle movement and in elastic energy storage during jet locomotion.

Received 13 December 2000; accepted 8 May 2001.

* To whom correspondence should be addressed. E-mail: joethomp@email.unc.edu

Abbreviations: DML, dorsal mantle length; IM-1, intramuscular fiber system 1; IM-1_{SAG}, sagittal component of IM-1 fiber angle; IM-1_{TAN}, tangential component of IM-1 fiber angle; IM-2, intramuscular fiber system 2.

Introduction

In the hydrostatic skeletons of soft-bodied invertebrates, the organization of connective tissue fibers is crucial for providing structural reinforcement, controlling shape, transmitting stresses, and storing elastic energy (*e.g.*, Harris and Crofton, 1957; Chapman, 1958; Clark and Cowey, 1958; Clark, 1964; Wainwright, 1970; Wainwright *et al.*, 1976; Wainwright and Koehl, 1976; Koehl, 1977; Gosline and Shadwick, 1983a). Though not particularly well documented for invertebrates, the organization of connective tissue fibers can change substantially during ontogeny (Cassada and Russell, 1975; Cox *et al.*, 1981). Such ontogenetic changes in the arrangement of connective tissue fibers may alter the functions and properties of the hydrostatic skeleton. The goal of this study is to examine the functional implications of ontogenetic changes in connective tissue fiber organization in a soft-bodied invertebrate.

Squid mantle morphology

Squid are soft-bodied molluscs that combine a hydrostatic skeleton with an uncalcified, chitinous gladius (= pen) to provide shape and structural support for the mantle. The mantle lacks the large, fluid-filled spaces characteristic of the hydrostatic skeleton of many worms and polyps. Instead, the muscle fibers and connective tissue fibers of the

mantle are packed into a dense, three-dimensional array. Water contained within the muscle fibers and the connective tissue fibers themselves serves as the incompressible fluid. In such a system of structural support, termed a "muscular hydrostat" by Kier and Smith (1985), the volume of the mantle remains constant, such that a change in one dimension must result in a change in at least one of the other dimensions of the mantle.

The mechanical support for the mantle arises from a complex, three-dimensional arrangement of muscle fibers, connective tissue fibers, and the gladius. The muscle fibers in squid mantle are arranged primarily in two orientations: circumferentially and radially. Contraction of the circumferential muscles decreases mantle circumference and expels water from the mantle cavity through the funnel during the exhalant phase of jet locomotion (Young, 1938). Contraction of the radial muscle fibers thins the mantle wall and increases the mantle circumference, filling the mantle cavity during the inhalant phase of jet locomotion (Young, 1938).

The fibrous connective tissues of the squid mantle are arranged into five networks (Fig. 1): the inner and outer tunics, which sandwich the circumferential and radial muscles, plus three networks of intramuscular collagen fibers (Ward and Wainwright, 1972; Bone *et al.*, 1981). Intramuscular fiber system 1 (IM-1) consists of collagen fibers (Gosline and Shadwick, 1983b; MacGillivray *et al.*, 1999) that originate and insert on the inner and outer tunics (Ward and Wainwright, 1972). Viewed in sagittal section, the IM-1 collagen fibers are arranged at a low angle (28° in *Lolliguncula brevis*) relative to the long axis of the mantle (Ward and Wainwright, 1972) (Fig. 1). In sections tangential to the surface of the mantle, the collagen fibers in IM-1 are also arranged at low angles (10° to 15° in *Alloteuthis subulata*) relative to the long axis of the mantle (Bone *et al.*, 1981) (Fig. 1). Thus, the IM-1 fibers actually follow an oblique path through the mantle wall, relative to both tangential and sagittal planes.

Intramuscular fiber system 2 (IM-2) is composed of collagen fibers (MacGillivray *et al.*, 1999) localized to the radial muscle bands (Bone *et al.*, 1981) (Fig. 1). Collagen fibers in IM-2 originate and insert on the inner and outer tunics and are arranged at an angle of about 55° to the mantle surface in *Alloteuthis subulata* (Bone *et al.*, 1981).

The final connective tissue fiber system in squid mantle is intramuscular fiber system 3 (IM-3). Collagen fibers (MacGillivray *et al.*, 1999) in IM-3 are arranged parallel to the circumferential muscle fibers and are not attached to the tunics (Bone *et al.*, 1981).

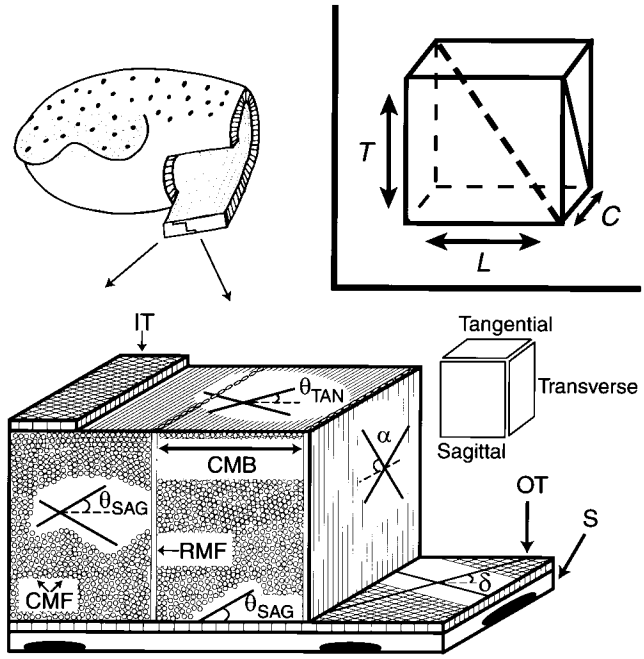

Figure 1. A schematic diagram illustrating mantle organization. The block of mantle tissue at the bottom left is from the ventral portion of the squid mantle at the upper left. The section planes are indicated immediately to the right of the block of tissue. Note that the IM-1 collagen fibers follow an oblique trajectory through the mantle. Thus, the fibers are seen in both the sagittal and tangential planes. IM-2 collagen fibers are restricted to radial muscle bands in the transverse plane. α, IM-2 fiber angle; δ, outer tunic fiber angle; θ_{SAG}, sagittal component of the IM-1 fiber angle; θ_{TAN}, tangential component of the IM-1 fiber angle; CMB, circumferential muscle band; CMF, circumferential muscle fibers; IT, inner tunic; OT, outer tunic; RMF, radial muscle fibers; S, skin. INSET. The inset at the top right of the figure is the polygon used to model the effect of ontogenetic changes in collagen fiber orientation on mantle kinematics and fiber strain. The solid gray line denotes an IM-2 collagen fiber, and the dashed gray line represents a single IM-1 collagen fiber. *C*, *L*, and *T* represent the circumferential direction, longitudinal direction, and thickness of the mantle wall, respectively. The circumference of the model (side *C*) was varied to simulate jet locomotion. See Discussion for additional details.

Mantle connective tissue function

The tunics and intramuscular collagen fibers serve important roles in controlling shape change in the mantle. The low fiber angles reported for tunic and IM-1 fibers in *Lolliguncula brevis* suggest strongly that the tunics and IM-1 help prevent mantle elongation during contraction of the circumferential muscles (Ward and Wainwright, 1972). This putative role is corroborated by Ward's (1972) observation that mantle length in *L. brevis* does not change measurably during jetting, though Packard and Trueman (1974) report small (*i.e.*, <5%) increases in *Loligo vulgaris* and *Sepia officinalis.*

The collagen fibers in IM-1 and IM-2 may resist the substantial increase in mantle thickness that occurs during circumferential muscle contraction. In addition, these collagen fibers are thought to store elastic energy during the exhalant phase of the jet and return that energy to help restore mantle shape and refill the mantle cavity (Ward and Wainwright, 1972; Bone *et al.*, 1981; Gosline *et al.*, 1983; Gosline and Shadwick, 1983a, b; Shadwick and Gosline,

1985; MacGillivray *et al.,* 1999; Curtin *et al.,* 2000). The IM-1 and IM-2 collagen fibers may also help restore mantle shape during the low-amplitude movements that occur during respiration (Gosline *et al.,* 1983).

Specific problem addressed

Virtually all the published work on squid mantle morphology and function is on adult loliginid squid. The few studies of hatchling or juvenile loliginid squid reveal dramatic changes in mantle function during ontogeny. For example, the morphology and physiology of the mantle musculature in *Photololigo* sp. and *Loligo opalescens* (Moltschaniwskyj, 1994; Preuss *et al.,* 1997) and the neuromuscular physiology underlying the escape response in *L. opalescens* (Gilly *et al.,* 1991) change significantly during growth from hatchlings to adults. Importantly for this study, the range of mantle movement during jet locomotion in newly hatched *L. opalescens* and *Loligo vulgaris* is greater than in adult animals (Packard, 1969; Gilly *et al.,* 1991; Preuss *et al.,* 1997). Given the link between the mantle connective tissue arrangement and mantle kinematics, it is likely that the orientation, the mechanical properties, or both the orientation and mechanical properties of squid mantle collagen change during ontogeny. Here, we examine ontogenetic changes in the arrangement and amount of connective tissue in the mantle in the oval squid, *Sepioteuthis lessoniana* (Cephalopoda: Loliginidae). The effect of ontogenetic changes in the collagen fiber arrangement of the outer tunic, IM-1, and IM-2 on mantle kinematics and elastic energy storage during jet locomotion is also analyzed.

Materials and Methods

Animals

We obtained an ontogenetic series of *Sepioteuthis lessoniana* Lesson, 1830. Wild embryos collected from three locations (Gulf of Thailand; Okinawa Island, Japan; Tokyo region, East Central Japan) over a 2-year period were reared (Lee *et al.,* 1994) by the National Resource Center for Cephalopods (NRCC) at the University of Texas Medical Branch (Galveston, TX). Each of the three cohorts consisted of thousands of embryos from six to eight different egg mops. Thus, it is likely that the sample populations were not the offspring of a few closely related individuals, but were representative of the natural population at each collection site.

Commencing at hatching, and at weekly intervals thereafter, live squid were sent *via* overnight express shipping from the NRCC to the University of North Carolina. The squid, which ranged from 5 mm to 70 mm in dorsal mantle length (DML), were killed by over-anesthesia in a solution of 7.5% $MgCl_2$ mixed 1:1 with artificial seawater (Messenger *et al.,* 1985). The $MgCl_2$ solution relaxed the mantle musculature of nearly all of the squid. Animals in which the mantle musculature was contracted noticeably were not used for the histological study. The $MgCl_2$ solution did not distort the shape of the mantle. The resting mantle diameter of an anesthetized squid was always 80% to 90% of the peak mantle diameter measured during jet locomotion in the same, unanesthetized animal (for details of the kinematics measurements, see Thompson and Kier, 2001).

Histology

The mantle tissue was examined using standard histological methods. Immediately after death, the squid were fixed whole in 10% formalin in seawater for 48 to 96 h at 20° to 23 °C. In the larger animals (>25 mm DML), the animal was decapitated to permit unrestricted flow of fixative into the mantle cavity. The mantles were fixed whole, rather than dissected into smaller blocks of tissue, to help minimize shape changes (*e.g.,* curling or bending of the tissue block) that could affect connective tissue fiber angle.

Following fixation, the tissue was dehydrated in a graded series of ethanol and cleared in Histoclear (National Diagnostics, Atlanta, GA) or Hemo-D (Fisher Scientific, Pittsburgh, PA). There was no discernible scale-related distortion of the mantle during dehydration and clearing. After clearing, the mantle was dissected into smaller pieces and embedded in paraffin (Paraplast Plus, Oxford Labware, St. Louis, MO; melting point 56 °C). To minimize shrinkage artifacts, infiltration with molten paraffin was limited to a total of 90 min (30-min baths × 3 changes) instead of the 180 min (60-min baths × 3 changes) recommended by Kier (1992).

Following clearing, most of the squid smaller than 30 mm DML were sliced in half along the sagittal plane using a fine razor blade. One half of the animal was oriented in the embedding mold to permit the cutting of sagittal sections; the other half was oriented for cutting of transverse sections. Many of the smaller squid were sliced in half along the frontal plane. The dorsal and ventral halves were oriented in the embedding molds to allow grazing sections to be cut. For the squid larger than 30 mm DML, large blocks of tissue of about 5 mm by 3 mm by the thickness of the mantle were dissected from several locations along the length and around the circumference of the mantle. These tissue blocks were oriented in the embedding molds to permit the cutting of sagittal, transverse, and tangential sections.

The tissue blocks were sectioned using a rotary microtome. The sections were mounted on slides coated with Mayer's albumin and stained with picrosirius stain (Sweat *et al.,* 1964; protocol adapted from López-DeLeón and Rojkind, 1985). Other connective tissue stains were used successfully (*e.g.,* Milligan trichrome, picro-ponceau, and van Gieson's stain) but picrosirius stain provided the best

contrast between the collagenous and non-collagenous components of the tissue sections and made identification of intramuscular collagen fibers straightforward.

Several additional attributes made picrosirius an excellent choice for this study. First, the sirius red F3B dye molecules attach with their long axes parallel to the long axes of the collagen fibrils, enhancing the natural birefringence of collagen fibers (Montes and Junqueira, 1988). Second, picrosirius is an outstanding stain for resolving the smallest collagen fibers and fibrils. The stain has been used previously to visualize the fine reticular collagen fibers present in embryonic mammalian skin and organs, the thin type-II collagen fibrils present in mammalian cartilage, and the extremely fine type-IV collagen fibrils present in mammalian basal laminae (Montes and Junqueira, 1988). Third, there is a strong correlation between the collagen volume fraction estimated from paraffin-embedded human liver sections using the picrosirius stain and the collagen volume fraction from the same tissue sections measured by hydroxyproline content analysis (López-DeLeón and Rojkind, 1985). Thus, picrosirius stain is ideal for both visualizing collagen fibers and making precise estimates of collagen volume fraction.

The stained sections were viewed using brightfield and polarized light microscopy. Fiber angles were measured from digital photomicrographic images using image analysis software (SigmaScan Pro, SPSS Science, Chicago, IL).

Initial survey

We made an initial survey of the mantle intramuscular fiber (IM) networks 1 and 2 in five squid (25 mm to 70 mm DML) to help develop a protocol for measuring IM fiber angles. In this survey, IM-1 and IM-2 fiber angles from different regions along the length and around the circumference of the mantle were examined. IM-1 and IM-2 fiber angles were measured at four positions along the length of the mantle (1/10, 1/4, 1/2, and 3/4 DML) and at three positions around the circumference of the mantle (ventral, lateral, dorsal). Given the potential for regional differences in IM fiber angle (see Results for details), all the comparisons among the squid were made at the same location: the ventral portion of the mantle between 1/3 and 2/3 DML.

IM-1 fiber angle measurements

IM-1 collagen fibers are arranged obliquely to the sagittal plane (Fig. 1). Therefore, to describe accurately the trajectory of these fibers, two fiber angles must be measured. The first angle, called IM-1_{SAG} here, is the angle of IM-1 collagen fibers relative to the long axis of the mantle in the sagittal plane (Fig. 1). The second angle, which we call IM-1_{TAN}, is the IM-1 fiber angle relative to the long axis of the mantle in a plane tangential to the outer surface of the mantle and perpendicular to the sagittal plane (Fig. 1).

IM-1_{SAG} fiber angle measurements

IM-1_{SAG} fiber angles were measured from sagittal sections (thickness 10–15 μm) of the mantle. Criteria were developed to ensure consistency across all squid in the ontogenetic series. First, all measurements of fiber angles were made from the ventral portion of the mantle between 1/3 and 2/3 DML. This eliminated errors due to variation in fiber angle along the length and around the circumference of the mantle.

Second, because the apparent fiber angle depends on the viewer's perspective, IM-1_{SAG} fiber angles were measured only from tissue sections in which the circumferential muscle fibers of the mantle were cut in nearly perfect cross section. This restriction ensured that the perspective was similar for all the squid examined. Adjusting the orientation of the tissue block relative to the microtome knife made it possible, through trial and error, to meet this criterion, and conformance was determined by examining test sections 20 μm thick.

Third, sagittal tissue sections contained IM-1 fibers of varying lengths. It was difficult to obtain accurate angle measurements of the shortest fibers in each section. Therefore, IM-1_{SAG} fiber angle measurements were made only on IM-1 fibers longer than the width of one circumferential muscle band. A circumferential muscle band was defined as a region of circumferential muscle fibers bounded by radial muscle fibers (Fig. 1).

Fourth, in all animals larger than about 15 mm DML, IM-1_{SAG} fiber angles were measured only from crossed IM-1 fibers. The angle between the two fibers was measured and the half angle reported as the IM-1_{SAG} fiber angle (Fig. 1). In squid smaller than 15 mm DML, IM-1 fibers were so scarce that there were few instances of crossed fibers. In these small squid, IM-1_{SAG} fiber angles were measured relative to the outer or the inner tunic (Fig. 1). In areas where the tunics were folded due to histological artifact, IM-1_{SAG} fiber angles were not measured.

Finally, the fiber angle of every IM-1_{SAG} fiber in a given microscope field that conformed to the criteria was measured. A minimum of 20 measurements was made from each squid larger than about 15 mm DML. Because IM-1 fibers were sparse in animals smaller than 15 mm DML, the minimum number of fiber angle measurements was eight in these animals.

IM-1_{TAN} fiber angle measurements

IM-1_{TAN} fiber angles were measured from relatively thick (10 to 15 μm) tangential sections of the mantle. To ensure consistency in fiber angle measurements among all squid, the criteria listed previously were used with two exceptions. First, IM-1_{TAN} fiber angles were measured only in those sections in which the radial muscle fibers were cut in nearly perfect cross section (determined from 20-μm

thick test sections). Second, for squid larger than about 15 mm DML, fiber angles were measured only from crossed IM-1 fibers. In the smallest squid (<15 mm DML), there were few IM-1 fibers and virtually no crossed fibers. In these squid, IM-1_{TAN} fiber angles were measured relative to a band of radial muscle fibers. Subtracting the measured angle from 90° gave the angle of the IM-1_{TAN} fiber relative to the long axis of the squid.

IM-2 fiber angle measurements

IM-2 fiber angles were measured from 5 μm thick transverse sections of the mantle. As with the IM-1 measurements, IM-2 fiber angles were measured only from the ventral portion of the mantle between 1/3 and 2/3 DML. Fiber angles were measured only from sections that were nearly perfect transverse sections of the mantle. Sections oblique to the transverse plane show circumferential muscle fibers in closely spaced bands separated by a few radial muscle fibers. Nearly perfect transverse sections exhibited uninterrupted circumferential muscle fibers. IM-2 fiber angle was measured only from crossed fibers (Fig. 1). Given the scarcity of IM-2 fibers in squid smaller than about 15 mm DML, it was not always possible to measure crossed fibers. In these small squid, IM-2 fiber angle was also measured relative to nearby radial muscle fibers. Finally, the fiber angle of every IM-2 fiber in the microscope field was measured. No fewer than 20 fiber angle measurements were made from each squid longer than about 15 mm DML. The relative paucity of IM-2 fibers in squid smaller than 15 mm DML reduced the minimum number of fiber angle measurements to eight per squid.

Outer tunic fiber angle measurements

Outer tunic fiber angles were measured from 5-μm-thick grazing sections of the mantle. Tunic fiber angles were measured only from the ventral portion of the mantle between 1/3 and 2/3 DML and only from crossed fibers. The half angle between the crossed tunic fibers, relative to the long axis of the squid, was reported as the fiber angle (Fig. 1). A minimum of 20 fiber angle measurements was made from each squid.

Stereology

Stereological methods were used to estimate the volume fraction of IM-1 and IM-2 collagen fibers relative to the volume of the mantle musculature. To obtain an accurate estimate of the volume fraction of a particular tissue component, stereology requires that the tissue of interest be sectioned in randomly oriented planes (Weibel, 1979). Because it is difficult to positively identify a collagen fiber in a random section plane as an IM-1 or IM-2 fiber, it was not possible to use random section planes. IM-1 collagen fiber volume fraction was therefore determined from sagittal sections of the ventral mantle in which fiber identity could be verified. Likewise, IM-2 collagen fiber volume fraction was measured from transverse sections of the ventral mantle. Although this violates an assumption of stereology, it allows accurate comparison of the relative volume fraction of collagen fibers among squid in the ontogenetic series. However, this method is inappropriate for estimation of the absolute volume fraction of collagen fibers in the mantle (Weibel, 1979).

The procedure for collagen volume fraction determination was similar for both IM-1 and IM-2. The ventral portion of the mantle between 1/3 and 2/3 DML was examined. A slide containing either sagittal (IM-1) or transverse (IM-2) 10-μm-thick tissue sections was placed on the stage of a compound microscope, and the tissue positioned under a 40× objective lens without observation through the oculars. The tissue section was brought into focus, and an image of the section was captured by a digital camera. The image was expanded to fill the screen of the monitor, and a transparent plastic overlay with a grid of 24 lines × 24 lines (Weibel, 1979) was taped to the screen. The intersection of a collagen fiber in IM-1 (sagittal sections only) or IM-2 (transverse sections only) with the junction of two lines (= a point; there were 24 lines × 24 lines = 576 points on the grid) was counted as a "hit." After the image was sampled, the microscope stage was moved haphazardly without observing the image through the microscope. In all cases, the stage was moved sufficiently far to ensure that the same portion of the mantle tissue was not examined twice. Another digital image was then captured, and the procedure was repeated at 2 or 3 different locations within the same tissue section and on between 3 and 10 different tissue sections per squid. The average volume fraction of collagen in IM-1 and IM-2 relative to the average volume of the mantle musculature was calculated by dividing the total number of hits by the total number of points counted for each squid (Weibel, 1979).

In stereology, both the acceptable standard error of the volume fraction estimate and the volume fraction of the item of interest determine the total number of points that must be counted (Weibel, 1979). The total number of points (P_C) was determined by

$$P_C = (t_\alpha^2/m_t d^2)*(1 - V_V/V_V) \quad \text{(Weibel, 1979)} \quad (1)$$

where m_t is the number of tissue sections examined per squid, d is the confidence interval, t_α is the acceptable error probability (the chance that the true volume fraction will be outside the confidence interval), and V_V is the volume fraction of the item of interest. To determine P_C, the volume fraction (V_V) of collagen in both IM-1 and IM-2 was estimated for four squid of various sizes (5 mm, 15 mm, 27 mm, and 69 mm DML) using the procedure outlined in the

Table 1

Comparison of the relative volume fraction of collagen in IM-1 and IM-2 among squid divided into the life-history stages of Segawa (1987)

Life-history stage	IM-1 points counted	IM-1 volume fraction	IM-2 points counted	IM-2 volume fraction
Hatchling ($n = 4$)	14,985 (14,265)	**0.00095** ± 0.0002	10,414 (9,504)	**0.0027** ± 0.0018
Juvenile 1 ($n = 4$)	6,516 (616)	**0.015** ± 0.0036	5,340 (647)	**0.027** ± 0.024
Juvenile 2 ($n = 4$)	4,344 (606)	**0.032** ± 0.012	3,258 (436)	**0.057** ± 0.021
Young 2 ($n = 4$)	3,801 (975)	**0.065** ± 0.036	3,258 (746)	**0.097** ± 0.024

The mean volume fraction of collagen is listed in boldface type ± the standard deviation of the mean. The total number of points counted for each individual squid is listed. The adjacent numbers in parentheses indicate the number of points that need to be counted ($=P_C$, see equation 1) to obtain an error probability of 5% and a confidence interval of ±10%. Within IM-1 and within IM-2, the volume fraction of collagen differed significantly among all life-history stages (one-way ANOVA on ranks, $P < 0.05$).

previous paragraph. Using the initial estimate of V_V, an error probability of 5%, and a confidence interval of ±10%, the total number of points to be counted (P_C) was calculated (Table 1). The V_V of collagen was strongly correlated with squid size. Thus, the total number of points counted per squid varied with size. Note that the actual number of points counted per squid was much greater than the minimum required to obtain an error probability of 5% and a confidence interval of ±10%. Thus, the actual error probability and confidence interval were smaller than the predicted values.

Statistical analysis

The sample population used in this study was subdivided into the life-history stages described by Segawa (1987). The life-history stages were selected as an independent organization scheme upon which to base the statistical analysis. Segawa (1987) studied the life cycle of *S. lessoniana* from embryo to adult and divided the life cycle into seven stages on the basis of morphological and ecological characters. These seven stages are hatchling (up to 10 mm DML), juvenile 1 (11–25 mm DML), juvenile 2 (26–40 mm DML), young 1 (41–60 mm DML), young 2 (61–100 mm DML), subadult (100–150 mm DML), and adult (>150 mm DML). The sample population of *S. lessoniana* used in the current investigation included the hatchling, juvenile 1, juvenile 2, and young 2 stages.

Nonparametric statistics were used for most of the analyses because the sample population was not normally distributed. For comparisons among the life-history stages, Kruskal-Wallis one-way analysis of variance on ranks was used with Dunn's method of pairwise multiple comparisons (Zar, 1996). All statistical analyses were completed using SigmaStat 1.01 (SPSS Science).

Results

General description of mantle morphology

The mantle of *Sepioteuthis lessoniana* is similar to that described for other loliginid squid (Young, 1938; Ward and Wainwright, 1972; Bone *et al.*, 1981). The outer tunic is located underneath the collagen-rich skin. The fibers within the outer tunic are robust and closely packed. The outer tunic serves as the insertion for the radial muscle fibers, the IM-1 collagen fibers, and the IM-2 collagen fibers. The fairly low-resolution microscopic methods used in this study did not permit a detailed examination of the connections between the outer tunic and the IM collagen fibers or the radial musculature.

The majority of the mantle is composed of circumferential muscle fibers. These muscle fibers are bordered by the outer and inner tunics and are partitioned by regularly spaced bands of radial muscle fibers. Consistent with the trend for *Photololigo* sp. (Moltschaniwskyj, 1994), the circumferential muscle fibers increased in diameter during ontogeny from 2.5 μm ± 0.49 μm (mean ± standard deviation, $n = 46$ from four specimens) in newly hatched squid to 3.9 μm ± 0.66 μm ($n = 43$ from four individuals) in the largest animals examined. In addition, the ratio of mitochondria-rich to mitochondria-poor (Bone *et al.*, 1981; Mommsen *et al.*, 1981) circumferential muscle fibers decreased from 1:5 in newly hatched squid to 1:7 in young 2 stage squid. The number of mitochondria-rich fibers adjacent to the inner tunic is twice that of the mitochondria-rich muscle fibers adjacent to the outer tunic in *S. lessoniana.*

The inner tunic is adjacent to the mantle musculature and to the thin epithelial lining of the mantle cavity. The radial muscle fibers and the collagen fibers in IM-1 and IM-2 insert on the inner tunic.

Initial survey

An initial survey of the mantle revealed that IM-1 fiber angle and IM-2 fiber angle differ both along the length and around the circumference of the mantle in an individual squid. In the ventral portion of the mantle, there were no significant differences in IM-1 fiber angle or in IM-2 fiber angle between 1/4 and 3/4 DML. However, IM-1 fiber angle was about 10° higher at 1/10 DML and about 10° lower between 3/4 DML and the posterior tip of the mantle. Similar differences in IM-1 fiber angle along the length of

the mantle were also noted in the lateral and dorsal regions. There was no correlation between mantle thickness at either 1/10 or 3/4 DML and the fiber angle at that location.

Between 1/4 and 3/4 DML, both IM-1 fiber angle and IM-2 fiber angle were about 10° lower in the dorsal region of the mantle than in either the lateral or ventral portions. Within an individual squid, there were no significant differences between the average IM-1 fiber angles or IM-2 fiber angles in the lateral or ventral portion of the mantle between 1/4 and 3/4 DML. Again, there was no apparent correlation between mantle thickness and fiber angle at a particular location around the circumference of the mantle.

The implications of these differences in collagen fiber arrangement are unclear. It is interesting, however, that MacGillivray *et al.* (1999) did not report significant differences in mantle mechanical properties either along the length or around the circumference of the mantle in *Loligo pealei.* It is possible that the differences in IM-1 and IM-2 fiber angle reported here for *S. lessoniana* are not present in *L. pealei.* Alternatively, such differences, if present, may not translate into significant differences in mantle mechanical properties.

IM-1 fiber ontogeny

IM-1 collagen fibers were scarce in newly hatched squid relative to older, larger animals (Fig. 2). Dozens of sagittal tissue sections from a hatchling squid could be searched without encountering a single IM-1 fiber. As the squid grew during ontogeny, IM-1 collagen fibers became increasingly numerous and robust (Fig. 2). The diameter of IM-1 fibers increased during ontogeny from 0.58 μm $\pm$ 0.060 μm standard deviation (SD; $n = 24$ from four individuals) in newly hatched squid to 0.68 μm $\pm$ 0.052 μm SD ($n = 37$ from three animals) in the young 2 stage squid.

IM-1 fiber angle changed dramatically during ontogeny (Fig. 2). IM-1_{SAG} fiber angle was between 26° and 33° in newly hatched animals and increased exponentially during growth from hatching to about 15 mm DML (Fig. 3A). IM-1_{SAG} fiber angle remained fairly constant (about 43°) in squid larger than 15 mm DML (Fig. 3A). A one-way ANOVA on ranks showed that while hatchling stage IM-1_{SAG} fiber angle was significantly lower than the fiber angle of squid in the other life-history stages examined ($P < 0.05$, Table 2), there were no significant differences in fiber angle among the juvenile 1, juvenile 2, and young 2 stage animals (Table 2).

IM-1_{TAN} fiber angle also changed substantially during ontogeny. IM-1_{TAN} fiber angle was highest in newly hatched animals (between 35° and 46°) and declined to about 28° in the largest squid examined (Fig. 3B). A one-way ANOVA on ranks indicated that hatchling stage IM-1_{TAN} fiber angle was significantly higher than the fiber angle in all older, larger animals ($P < 0.05$, Table 2). There were no significant differences in IM-1_{TAN} fiber angle among the squid in the juvenile 1, juvenile 2, and young 2 life-history stages (Table 2).

IM-2 fiber ontogeny

IM-2 collagen fibers were scarce in newly hatched animals when compared to the older, larger squid in the study (Fig. 4). As with IM-1 fibers, many mantle tissue sections could be observed without locating a single IM-2 collagen fiber. However, IM-2 fibers increased in abundance and diameter as the squid grew during ontogeny (Fig. 4). The diameter of IM-2 collagen fibers increased from an average of 0.54 μm $\pm$ 0.080 μm SD ($n = 28$ from four animals) in newly hatched squid to an average of 0.71 μm $\pm$ 0.087 μm SD ($n = 31$ from three specimens) in the young 2 stage animals.

IM-2 fiber angle changed significantly during ontogeny (Fig. 4). IM-2 fiber angle was between 27° and 36° in newly hatched squid and rose exponentially until the squid grew to 15 mm DML (Fig. 3C). In squid larger than 15 mm DML, IM-2 fiber angle ranged between 48° and 58° (Fig. 3C). A one-way ANOVA on ranks showed that IM-2 fiber angle was lower in hatchling stage squid than in all older, larger animals ($P < 0.05$, Table 2). The one-way ANOVA on ranks also revealed that the IM-2 fiber angle in the juvenile 2 stage squid was marginally higher than in the juvenile 1 stage animals ($P = 0.05$, Table 2). There were no significant differences in IM-2 fiber angle between juvenile 1 and young 2 stage animals.

Outer tunic fiber ontogeny

Regardless of size, all the squid possessed a robust outer tunic (Fig. 5). The collagen fibers constituting the outer tunic changed in orientation during ontogeny. The outer tunic fiber angle was highest in newly hatched animals (between 27° and 36°) and declined during ontogeny (Fig. 3D). In squid larger than about 15 mm DML, outer tunic fiber angle decreased slightly with size from about 26° to 16° (Fig. 3D). A one-way ANOVA on ranks showed that the outer tunic fiber angle was higher in hatchling stage animals than in all older, larger squid ($P < 0.05$, Table 2). In addition, outer tunic fiber angle was slightly higher in juvenile 2 stage animals than in either juvenile 1 or young 2 stage animals ($P = 0.05$, Table 2). There were no significant differences in outer tunic fiber angle between juvenile 1 and young 2 stage squid.

Volume fraction of collagen in IM-1 and IM-2

Relative to the volume of mantle musculature, the volume fraction (V_V) of collagen in both IM-1 and IM-2 increased nearly 2 orders of magnitude during ontogeny (Fig. 6, Table 1). The volume fraction of collagen in IM-1

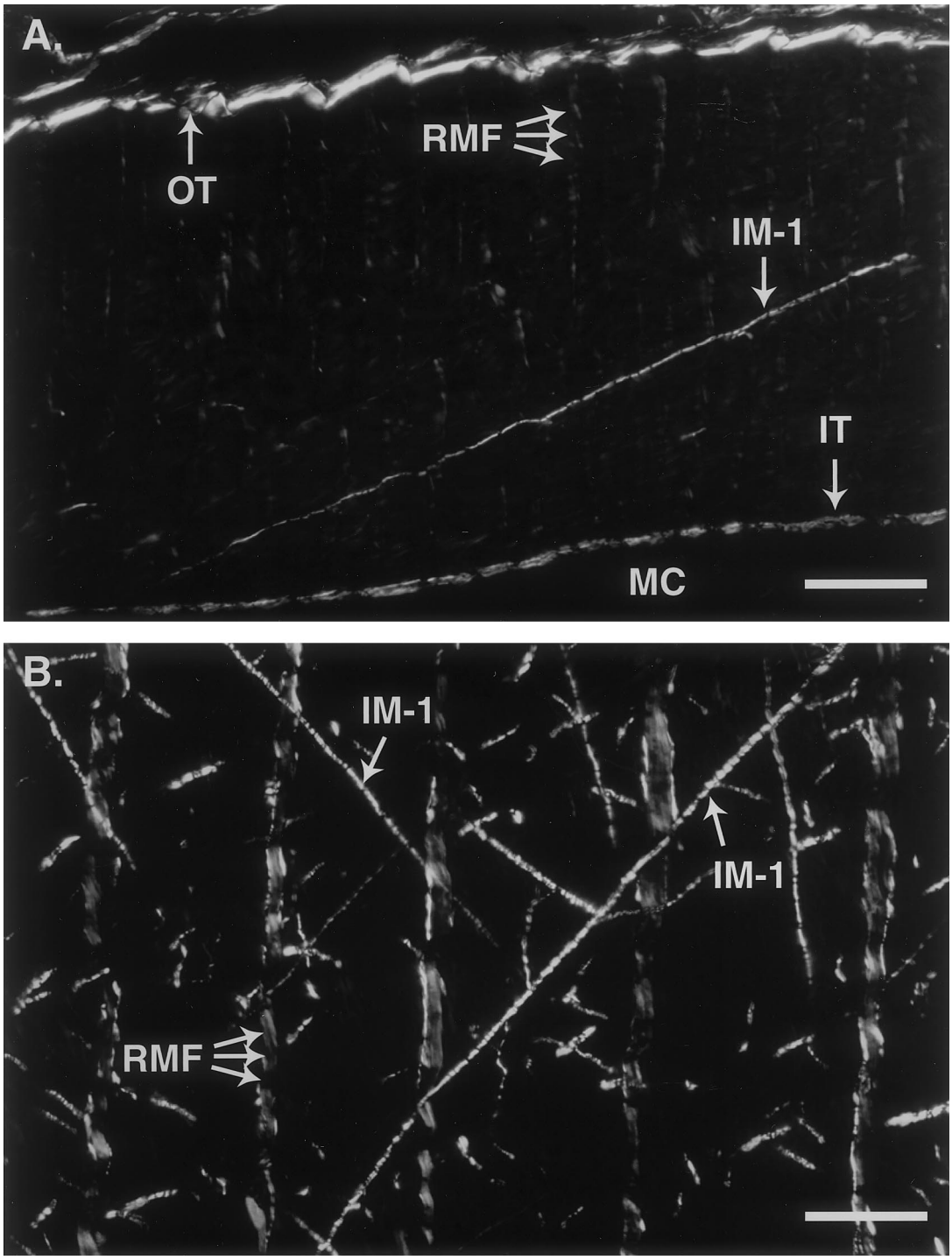

Figure 2. Photomicrographs (polarized light microscopy) of 5-μm-thick sagittal sections of the ventral mantle that illustrate ontogenetic differences in IM-1 collagen fibers. Sections were stained with picrosirius. The orientation of the mantle in both panels is identical. IM-1, intramuscular fiber system 1 collagen fiber; IT, inner tunic; MC, mantle cavity; OT, outer tunic; RMF, radial muscle band. Scale bar in A and B, 20 μm. (A) The ventral mantle of a newly hatched squid (DML, 5.5 mm) with a single IM-1 collagen fiber. The section is oblique to the sagittal plane. (B) The ventral mantle of a young 2 stage squid (DML, 65 mm). Note the low IM-1 collagen fiber angle and the absence of other IM-1 collagen fibers in the field of view in the hatchling squid. In the larger squid, IM-1 fiber angles are higher, and IM-1 collagen fibers are abundant.

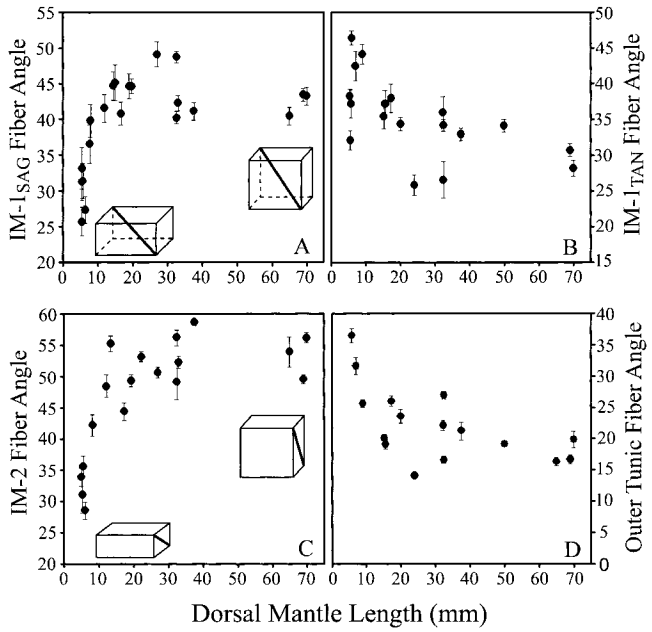

Figure 3. Ontogenetic changes in organization of mantle connective tissue. In all panels, each data point represents the mean of between 8 and 20 fiber angle measurements for one squid. The bars indicate the standard error of the mean. (A) Sagittal component of the IM-1 fiber angle *versus* dorsal mantle length (DML). IM-1_{SAG} is lowest in newly hatched squid and rises exponentially during growth up to 15 mm DML. In squid larger than 15 mm DML, IM-1_{SAG} does not change significantly. The block at the lower left illustrates the lower IM-1_{SAG} and higher IM-1_{TAN} fiber angles of a hatchling (see inset in Fig. 1 for orientation). The block at upper right illustrates the higher IM-1_{SAG} and lower IM-1_{TAN} fiber angles of an older, larger squid. (B) Tangential component of IM-1 fiber angle *versus* DML. IM-1_{TAN} is highest in newly hatched squid and declines during growth. (C) IM-2 fiber angle *versus* DML. IM-2 fiber angle is lowest in hatchlings and rises exponentially during growth up to 15 mm DML. In squid larger than 15 mm DML, IM-2 fiber angle increases slightly. The block at the lower left illustrates the lower IM-2 fiber angle in hatchlings. The block at the upper right illustrates the higher IM-2 fiber angle of larger squid. (D) Outer tunic fiber angle *versus* DML. Outer tunic fiber angle is highest in hatchlings and declines during ontogeny.

increased 68 times, from an average of 0.00095 in newly hatched squid to an average of 0.065 in the largest animals examined in this study (Table 1). A one-way ANOVA on ranks indicated that the volume fraction of collagen in IM-1 was significantly different among all the life history stages ($P < 0.05$, Table 1).

The volume fraction of collagen in IM-2 increased 36 times, from an average of 0.0027 in newly hatched animals to an average of 0.097 in the largest squid studied (Fig. 6, Table 1). A one-way ANOVA on ranks showed that the volume fraction of collagen was significantly different among all the life history stages examined ($P < 0.05$, Table 1).

Discussion

Connective tissue fibers limit the range of movement in many soft-bodied, cylindrical animals that rely upon a hydrostatic skeleton for support (*e.g.*, Harris and Crofton, 1957; Chapman, 1958; Clark and Cowey, 1958; Clark, 1964). The collagen fibers in the outer tunic, IM-1, and IM-2 may also affect the limits of mantle movement during jet locomotion. Because the fiber angles in all of the connective tissue fiber networks examined here change significantly during ontogeny, the kinematics of mantle movement probably change significantly as well.

The outer tunic

The tunics of squid are hypothesized to restrict mantle lengthening during jet locomotion (Ward and Wainwright, 1972). This important function ensures that the mechanical work performed by the circumferential musculature is used to decrease mantle cavity volume, thereby forcing water out of the funnel and producing thrust, instead of lengthening the mantle. The average outer tunic fiber angle of 17.7° from young 2 stage *Sepioteuthis lessoniana* was substantially

Table 2

Comparison of mantle collagen fiber organization among squid divided into the life-history stages of Segawa (1987)

Life-history stage	IM-1_{SAG} fiber angle	IM-1_{TAN} fiber angle	IM-2 fiber angle	Tunic fiber angle
Hatchling	**32.7** ± 9.22 (6)	**39.0** ± 6.37 (5)	**34.6** ± 6.76 (5)	**33.5** ± 6.37 (3)
Juvenile 1	**43.7** ± 7.33 (7)	**33.2** ± 6.74 (5)	**49.7** ± 6.52 (5)*	**20.6** ± 6.74 (5)
Juvenile 2	**43.2** ± 6.29 (5)	**32.8** ± 6.59 (4)	**53.9** ± 6.00 (5)*	**22.4** ± 6.59 (5)*
Young 2	**42.3** ± 6.50 (3)	**31.9** ± 3.65 (3)	**53.3** ± 5.40 (3)	**17.7** ± 3.65 (3)*

The mean fiber angle is listed in boldface type in each column ± the standard deviation of the mean. The number of squid in the sample is in parentheses. Each mean fiber angle was calculated from between 8 and 25 measurements of fiber angle for each squid in the sample. All the fiber angle measurements for each squid in a life-history stage were pooled to calculate the mean and the standard deviation. In each column, the mean fiber angle for the hatchling stage squid was significantly different from the mean fiber angle for the juvenile 1, juvenile 2, and young 2 life-history stages (one-way ANOVA on ranks, $P < 0.05$). The asterisks in the IM-2 fiber angle column indicate significant differences in mean fiber angle between the juvenile 1 and juvenile 2 life-history stages (one-way ANOVA on ranks, $P = 0.05$). The asterisks in the tunic fiber angle column indicate a significant difference in mean fiber angle between the juvenile 2 and young 2 life-history stages (one-way ANOVA on ranks, $P = 0.05$). Other within-column comparisons of fiber angle were not significantly different.

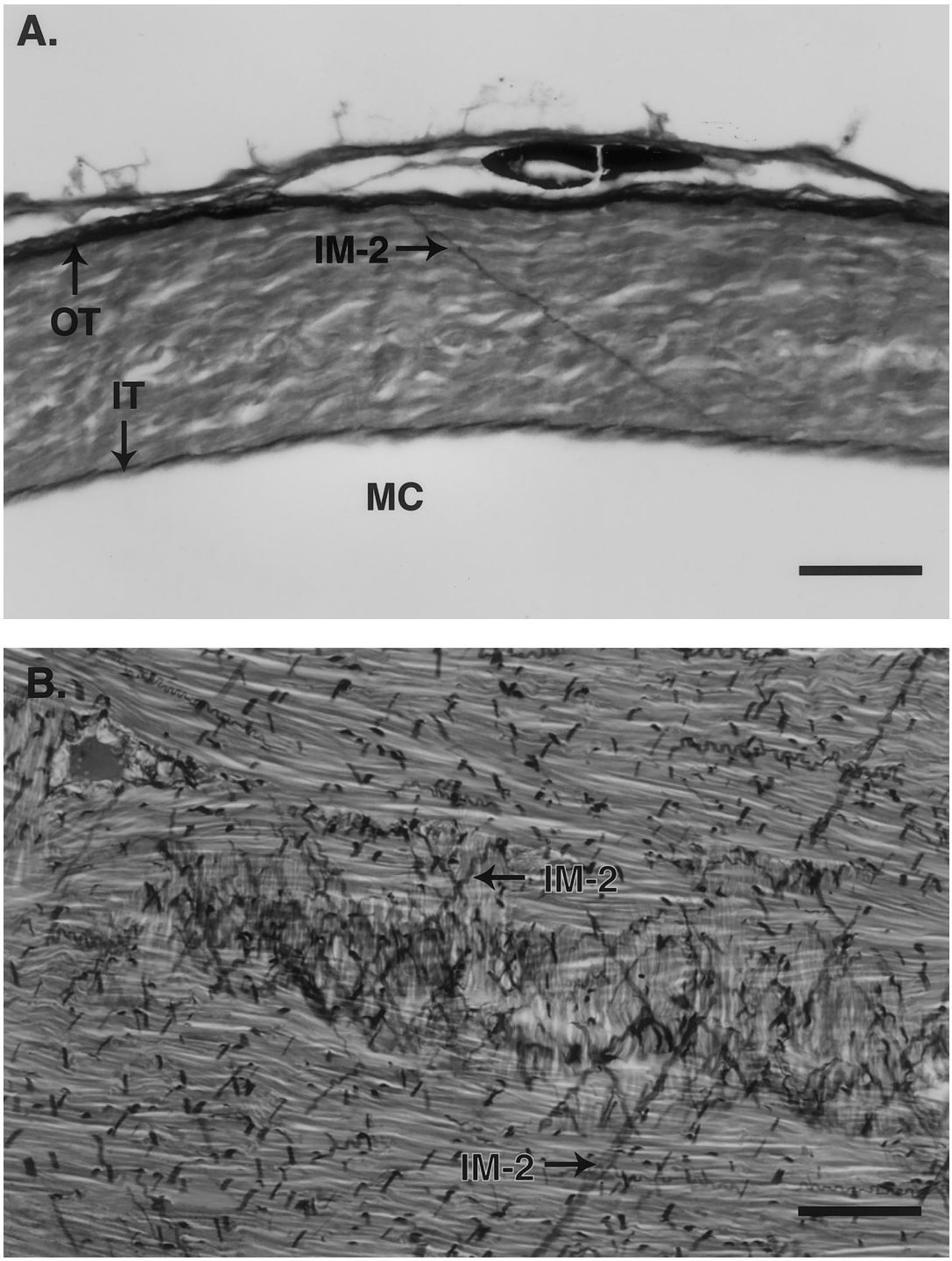

Figure 4. Photomicrographs (brightfield microscopy) of 10-μm-thick transverse sections of the ventral mantle that illustrate ontogenetic differences in IM-2 collagen fibers. Sections were stained with picrosirius. The orientation of the mantle is identical in both images. IM-2, intramuscular fiber system 2 collagen fiber; IT, inner tunic; MC, mantle cavity; OT, outer tunic. Scale bar in A and B, 60 μm. (A) A single IM-2 collagen fiber in a newly hatched squid (DML, 5 mm). Note the low IM-2 fiber angle and the scarcity of other IM-2 collagen fibers in the field of view. (B) IM-2 collagen fibers in the ventral mantle of a young 2 stage squid (DML, 69 mm). The faint vertical fibers near the center of the image are radial muscle fibers. Note that the IM-2 fiber angle is higher and IM-2 collagen fibers are abundant.

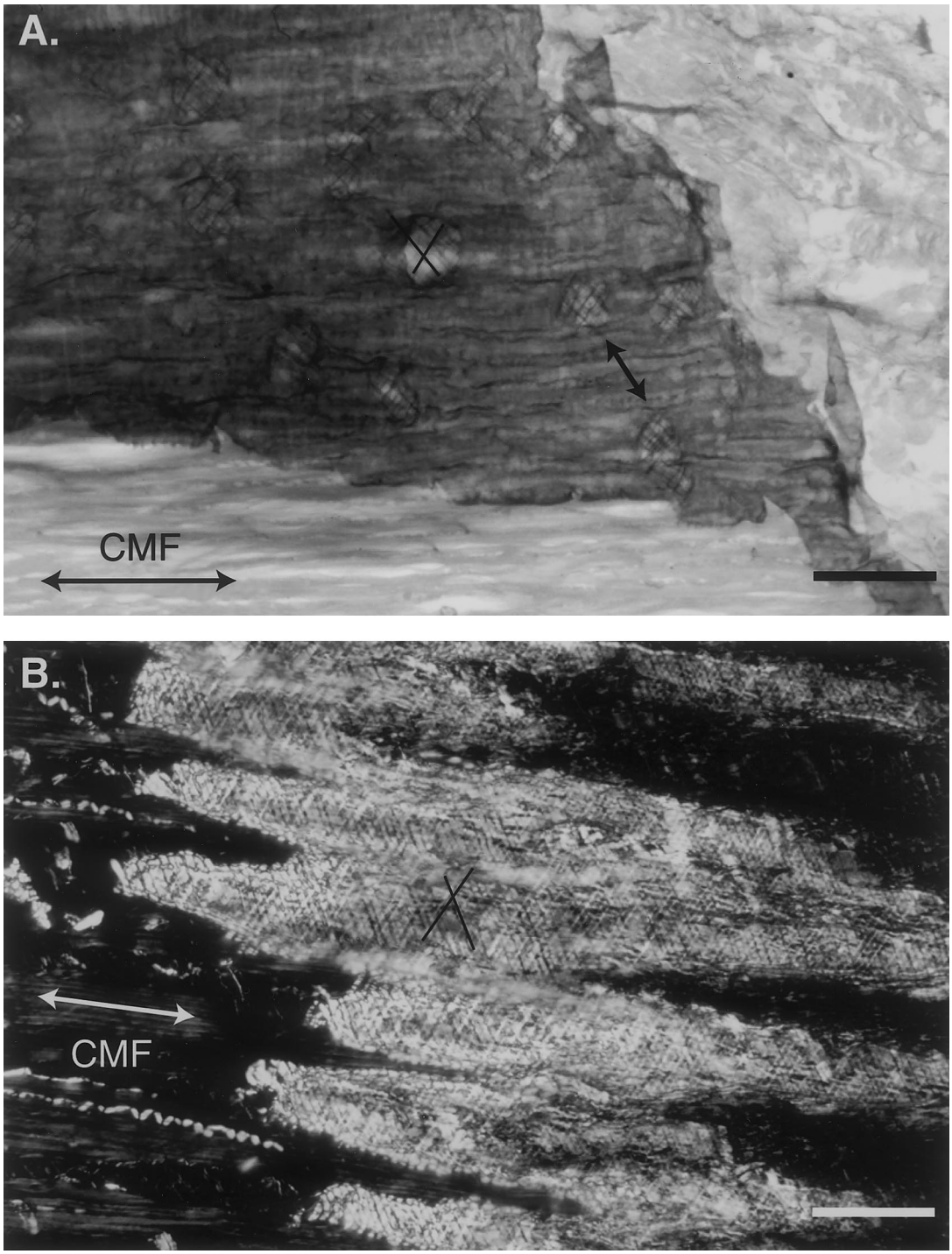

Figure 5. Photomicrographs of 5-μm-thick grazing sections of ventral squid mantle that illustrate the ontogenetic change in outer tunic collagen fiber angle. Black lines overlay a pair of collagen fibers in A and B to help illustrate the fiber angle. CMF, circumferential muscle fibers. Scale bars, 20 μm. (A) Outer tunic collagen fibers in a newly hatched squid (DML, 6 mm). Brightfield microscopy with picrosirius stain. The small arrow indicates additional outer tunic collagen fibers. (B) Outer tunic collagen fibers in a juvenile 2 stage squid (DML, 38 mm). Polarized light microscopy with picrosirius stain. Note the higher fiber angle in the hatchling animal.

lower than the 27° average outer tunic fiber angle reported for *Lolliguncula brevis* and *Loligo pealei* by Ward and Wainwright (1972). Indeed, the outer tunic fiber angle measured for mature *L. brevis* and *L. pealei* by Ward and Wainwright (1972) is much closer to the hatchling stage outer tunic fiber angle of 33.5° in *S. lessoniana.*

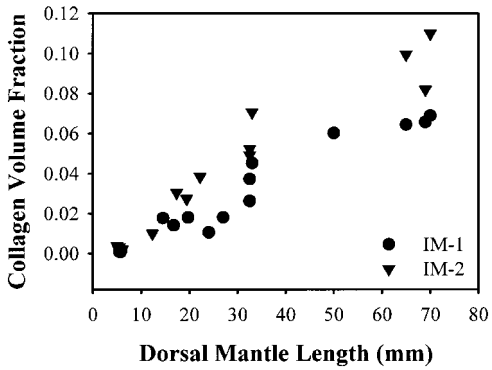

Figure 6. Collagen volume fraction in the ventral mantle *versus* dorsal mantle length. Each point represents the volume fraction of collagen for one squid. Circles indicate the volume fraction of collagen in IM-1, and triangles indicate the volume fraction of collagen in IM-2. The IM-2 data points obscure the IM-1 data for the hatchling stage squid.

The outer tunic fibers of all the *S. lessoniana* studied are oriented appropriately to resist lengthening of the mantle during jet locomotion (see Chapman, 1958, and Clark and Cowey, 1958). Both the mechanical properties and fiber angle of outer tunic collagen fibers affect mantle lengthening during jet locomotion. If the mechanical properties of the outer tunic collagen fibers do not change during ontogeny, the ability of the outer tunic to resist increases in mantle length during jet locomotion will depend on fiber angle. For example, if the maximum extensibility of an outer tunic collagen fiber is 0.13, a realistic assumption based on mechanical tests of squid mantle collagen (Gosline and Shadwick, 1983b), the mantle length of a hatchling stage squid may increase up to 23% during a jet whereas the mantle length of a young 2 stage animal may increase up to 17%. Thus, the ontogenetic variation in outer tunic fiber angle may allow greater mantle length increases during jet locomotion in newly hatched squid than in older, larger squid.

The possible increases in mantle length calculated above for *S. lessoniana* probably represent maximal values. The force balance between the outer tunic collagen fibers, other networks of connective tissue fibers, the chitinous gladius, and perhaps, the collagen-rich skin may all serve to limit changes in mantle length. The purpose of the calculation is simply to highlight the influence of outer tunic fiber angle on the *potential* for increases in mantle length during jet locomotion. Indeed, Ward (1972) did not observe increases in mantle length during jet locomotion in *L. brevis.* Packard and Trueman (1974), however, did notice small increases (~5%) in the ventral mantle length of subadult *Loligo vulgaris* and adult *Sepia officinalis.* As the next section illustrates, small increases in mantle length during the jet may facilitate elastic energy storage in the IM-1 collagen fibers of newly hatched *S. lessoniana.*

IM-1

Previous reports of IM-1_{SAG} fiber angle from *Lolliguncula brevis* and *Loligo pealei* are about 15° lower than the fiber angle reported here for the young 2 stage *S. lessoniana* (Ward and Wainwright, 1972). The discrepancy may be due to species differences or to the histological methods selected for the analysis. It is also possible that age or size differences may account for the disparity because mature squid were analyzed in the previous study. It is not possible to compare the IM-1_{SAG} hatchling fiber angle because, to our knowledge, there are no published values for newly hatched squid.

Bone *et al.* (1981) reported IM-1_{TAN} fiber angle data for *Alloteuthis subulata* and *Loligo forbesi.* In both species, the IM-1_{TAN} fiber angle was 15° to 20° lower than the angle measured here for young 2 stage *S. lessoniana.* The fiber angle reported by Bone *et al.,* however, was measured in partially contracted specimens. Contraction of the mantle results in a decrease of the IM-1_{TAN} fiber angle. Histological methodology, species differences, or age/size differences may also account for the disparity between the published fiber angle data and this study.

The significant ontogenetic change in IM-1_{SAG} and IM-1_{TAN} fiber angle may affect the kinematics of mantle movement during jet locomotion. To explore this idea, we developed a three-dimensional geometric model to evaluate the influence of changes in fiber angle on mantle kinematics. The model consists of a right rectangular polygon of mantle tissue (inset in Fig. 1). A single IM-1 collagen fiber extends from the front lower right corner to the rear upper left corner of the polygon (the gray dashed line in Fig. 1). The long axis of the polygon is parallel to the long axis of the mantle, and the short axis (side *C*) is parallel to the circumferential muscle fibers. The height of the polygon (side *T*) represents the thickness of a portion of the mantle wall. The dimensions of the polygon are in arbitrary units.

The polygon is assumed to have constant volume, and the IM-1 fiber is free to reorient as the polygon changes in dimensions. The short axis (side *C*, Fig. 1) of the polygon was decreased to simulate circumferential muscle contraction during jet locomotion. IM-1_{SAG} and IM-1_{TAN} average fiber angles from hatchling and young 2 stage *S. lessoniana* (see Table 2) were used as the initial condition (*i.e.,* "resting" mantle circumference) in which strain in the IM-1 fiber was assumed to be zero. Initially, the mantle length was held constant during the simulations. The strain on the IM-1 fiber and the IM-1_{SAG} and IM-1_{TAN} fiber angles were then calculated for a range of mantle circumference changes (see Appendix for a sample calculation).

The model predicts the effects of changes in IM-1 fiber angle on mantle kinematics. If mantle length is held constant during the jet cycle and if an IM-1 collagen fiber extensibility of 0.13 is assumed (Gosline and Shadwick,

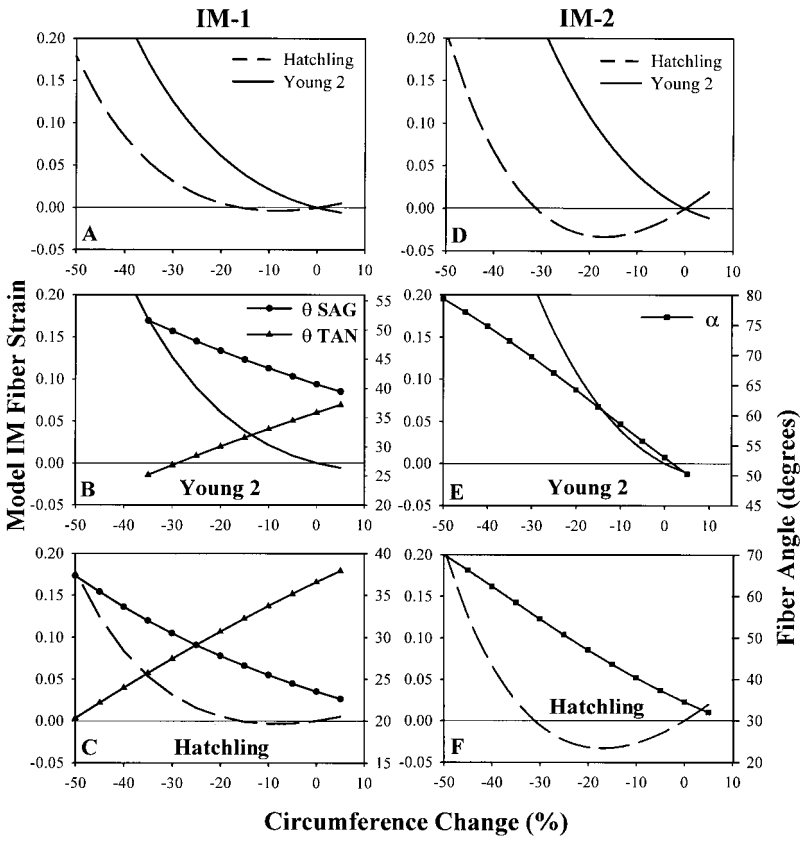

Figure 7. Predicted ontogenetic differences in collagen fiber strain and fiber angle during jet locomotion. The plots in the left column are for model IM-1 collagen fibers; the plots in the right column are for model IM-2 collagen fibers. The horizontal axis in each plot is the mantle circumference change that occurs during a simulated jet. Zero indicates the resting mantle circumference in an anesthetized squid. Negative numbers indicate mantle contraction, and positive numbers denote expansion of the mantle. The left vertical axis in each plot indicates strain on the model collagen fiber. The positive strain values above the horizontal zero line indicate lengthening of the model collagen fiber; the negative values below the zero line indicate compression. The right vertical axis in plots B, C, E, and F indicate the fiber angle of the model collagen fiber. The dashed lines represent strain data for the hatchling stage model and solid lines represent strain data for the young 2 stage model. Lines with symbols indicate the fiber angle predictions. (A and D) IM-1 fiber strain and IM-2 fiber strain, respectively, during a simulated jet. Mantle length was held constant during the simulated jet. Strain is lower at a given mantle circumference in the IM-1 and IM-2 hatchling stage model collagen fibers during the simulated jet than in the young 2 stage collagen fibers. In both A and D, if the maximum extensibility of the model collagen fibers remains unchanged during ontogeny, hatchling stage squid will experience much greater mantle contraction during the simulated jet than the young 2 squid. The hatchling fiber is compressed during the initial 17% of the mantle contraction in the IM-1 model and during the initial 32% of mantle contraction in the IM-2 model. Consequently, storage of strain energy in the model IM-1 and IM-2 collagen fibers is not possible unless the mantle contracts more than 17% and 32%, respectively. (B and C) Predicted changes in the sagittal (θ_{SAG}) and tangential (θ_{TAN}) components of the IM-1 fiber angle for a young 2 and a hatchling stage squid, respectively. In each case, note that θ_{SAG} increases while θ_{TAN} decreases during the simulated jet. (E and F) Predicted changes in the IM-2 fiber angle (α) for a young 2 and a hatchling stage squid, respectively. The fiber angle increases during the simulated jet in both cases.

1983b), the range of possible mantle movements changes substantially during ontogeny. In the model of the hatchling stage *S. lessoniana*, mantle circumference may decrease about 45% (Fig. 7A) during jet locomotion, whereas the mantle circumference of a young 2 stage animal may decrease only about 30% (Fig. 7A). In both hatchling and young 2 stage squid, the models show that IM-1_{SAG} fiber angle increases during the jet, while IM-1_{TAN} fiber angle decreases (Fig. 7B, 7C). It is also interesting to note that the low initial IM-1_{SAG} fiber angle and the high initial IM-1_{TAN} fiber angle in hatchling stage squid result in IM-1 fiber compression during the initial −17% mantle circumference change (Fig. 7A). If mantle length is constant during the jet, low-amplitude movements (*i.e.*, less than a 17% decrease in

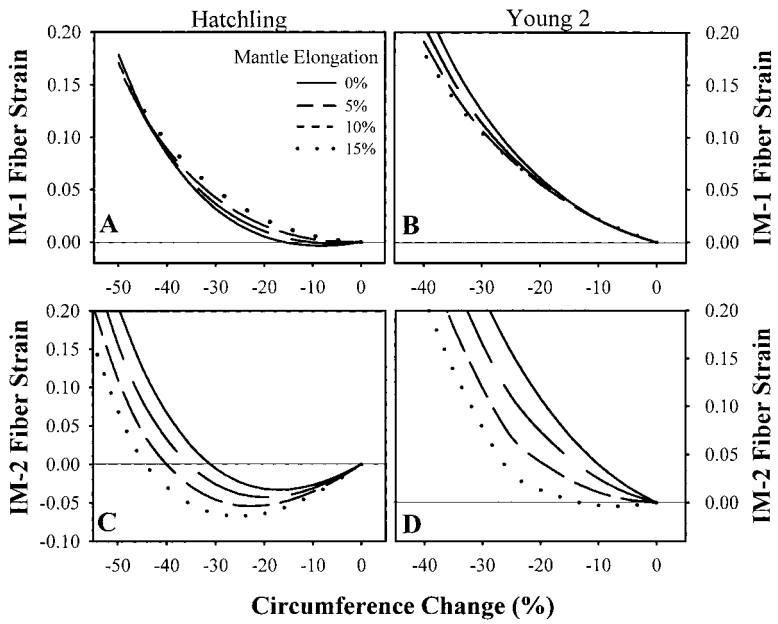

Figure 8. The effect on collagen fiber strain of an increase in mantle length during simulated jet locomotion. The plots in the left column are for the hatchling stage models; plots in the right column are for the young 2 stage models. The horizontal axis in each plot is the change in mantle circumference that occurs during a simulated jet. Zero indicates the resting mantle circumference in an anesthetized squid. Negative numbers indicate mantle contraction. The vertical axis in each plot indicates strain on the model collagen fiber. The positive strain values above the horizontal zero line indicate elongation of the model collagen fiber; the negative values below the zero line indicate compression. The amount of mantle elongation during the simulated jet in each graph is indicated in the legend for graph A. (A) Predicted IM-1 fiber strain in a hatchling stage squid. Increases in mantle length result in higher strain on the model collagen fiber early in the simulated jet stroke but do not greatly influence the possible range of mantle kinematics. (B) Predicted IM-1 fiber strain in a young 2 stage squid. Increases in mantle length do not affect strain on the model collagen fiber early in the simulated jet but do increase the possible range of mantle kinematics. (C and D) Predicted IM-2 fiber strain in a hatchling stage and a young 2 stage squid, respectively. Increases in mantle length during the simulated jet stroke substantially affect the possible range of mantle kinematics and the strain of the model IM-2 collagen fibers.

mantle circumference) of the mantle will not store strain energy in IM-1 collagen fibers in newly hatched squid.

We also examined the effect of mantle length increase during jet locomotion on mantle kinematics using the model. For both the hatchling and young 2 stage models, mantle length was allowed to increase 5%, 10%, and 15% during the jet cycle. In the hatchling stage model, mantle length was increased steadily until a mantle circumference change of −45% was reached (*i.e.*, the point in the previous IM-1 hatchling model where strain on the IM-1 collagen fiber was 0.13). In the young 2 stage model, mantle length was increased gradually until a mantle circumference change of −30% was reached (*i.e.*, the point in the previous IM-1 young 2 model where the strain on the IM-1 collagen fiber was 0.13). After mantle circumference changes of −45% for the hatchling stage model and −30% for the young 2 stage model were reached, mantle length was held constant. Note that incorporating the increases in mantle length earlier in the jetting cycle (*e.g.*, up to a mantle circumference change of −20%, then holding mantle length constant) does not affect the predicted maximum range of mantle contraction, though it does result in higher strain in the hatchling stage model IM-1 collagen fiber early in the jetting cycle. In all the simulations, the strain on the IM-1 fiber was calculated for a range of mantle circumference changes.

Incorporating mantle length increase during jet locomotion into the model results in several interesting predictions. In hatchling stage *S. lessoniana*, modest increases in mantle length during the jet did not substantially affect the maximum possible amplitude of mantle contraction, but they did result in an increase in IM-1 collagen fiber strain during low-amplitude mantle movements (Fig. 8A). The potentially important consequence of small increases in mantle length during jetting for newly hatched squid is that strain energy storage in IM-1 collagen fibers is possible during low-amplitude movements of the mantle (*e.g.*, respiration and slow jet locomotion). In the young 2 stage squid, only the 15% increase in mantle length during jet locomotion had any noticeable effect on IM-1 collagen fiber strain (Fig. 8B). The maximum possible mantle circumference change during the jet, however, increased slightly with modest in-

creases in mantle length (Fig. 8B). Thus, the model predicts that small increases in mantle length during low-amplitude mantle movements (*e.g.*, slow jetting or respiration) in newly hatched *S. lessoniana* may result in increased energy storage in IM-1 collagen fibers; small increases in mantle length in older, larger squid do not. The predicted increase in elastic energy storage comes at the expense of a decrease in thrust. For slow jetting or respiration, this cost may not outweigh the benefits of elastic energy storage.

IM-2

The average IM-2 fiber angle of young 2 stage *S. lessoniana* was about the same as the 55° reported for *Alloteuthis subulata* and *Loligo forbesi* by Bone *et al.* (1981). It is not possible to compare the average IM-2 fiber angle of the hatchling stage *S. lessoniana* with the literature because we are not aware of any published IM-2 fiber angles in newly hatched squid.

The significant change in IM-2 fiber angle during ontogeny may contribute to substantial ontogenetic changes in mantle kinematics during jet locomotion. We examined the implications of a fiber angle change on mantle kinematics using a model similar to the one used to predict the effect of IM-1 collagen fiber angle on mantle kinematics. The IM-2 model consists of the same polygon mentioned above, except there is a single IM-2 fiber running from the lower right corner to the upper left corner of plane *CT* (solid gray fiber in plane *CT*, Fig. 1). The assumptions are the same for both the IM-1 and IM-2 models.

The model predicts the potential effects of an ontogenetic change in IM-2 fiber angle on mantle kinematics. If the extensibility of the IM-2 collagen fiber in the model is limited to 0.13 (Gosline and Shadwick, 1983b), a mantle circumference change of about −45% is possible in hatchling stage *S. lessoniana* during jet locomotion (Fig. 7D). During mantle contraction, the hatchling IM-2 fiber angle will increase from about 35° to about 67° (Fig. 7F). Due to the low initial fiber angle, the IM-2 collagen fiber is compressed during the first −32% change in mantle circumference (Fig. 7D). The model predicts that strain energy storage in the IM-2 collagen fibers will occur only during vigorous jet locomotion that results in large decreases (>32%) in mantle circumference. Interestingly, this suggests that if hatchling stage *S. lessoniana* use elastic mechanisms to restore mantle shape during respiratory movements of the mantle, as hypothesized for mature *Loligo opalescens* by Gosline *et al.* (1983), strain energy storage can only take place in the IM-1 collagen fibers.

The model predicts substantially different mantle kinematics for young 2 stage *S. lessoniana.* Again, if IM-2 collagen fiber extensibility is assumed to be 0.13, mantle circumference changes during jet locomotion of up to about −25% are possible (Fig. 7D). The fiber angle will increase from the initial value of 53° to about 65° at the end of the jet (Fig. 7E). Given the high initial fiber angle, the strain experienced by the IM-2 collagen fibers will increase rapidly during the jet (Fig. 7D).

Because the mantle tissue is probably constant in volume over the brief period of a single mantle contraction (Ward, 1972), increases in mantle length during jet locomotion will influence the strain experienced by the IM-2 collagen fibers. Therefore, we also examined the effect of mantle length increase during jet locomotion on mantle kinematics. Mantle length in both the hatchling and young 2 stage models was allowed to increase 5%, 10%, and 15% during the jet cycle. In the hatchling stage model, mantle length was increased gradually until a mantle circumference change of −45% was reached (*i.e.*, the point in the previous hatchling IM-2 model where strain on the IM-2 collagen fiber was 0.13). In the young 2 stage model, mantle length was increased progressively until a mantle circumference change of −25% was reached (*i.e.*, the point in the previous young 2 IM-2 model where strain on the IM-2 collagen fiber was 0.13). Mantle length was held constant after mantle circumference changes of −45% and −25%, for the hatchling and young 2 stage models respectively, were reached. The strain on the IM-2 fiber was calculated for a range of changes in mantle circumference.

The models predict substantial effects on both mantle kinematics and elastic energy storage when mantle length increases during jet locomotion. The hatchling stage model predicts that modest 5% or 10% increases in mantle length during jetting increase proportionately the range of possible mantle circumference changes (Fig. 8C). Increases in the maximum amplitude of mantle movements during jet loco-

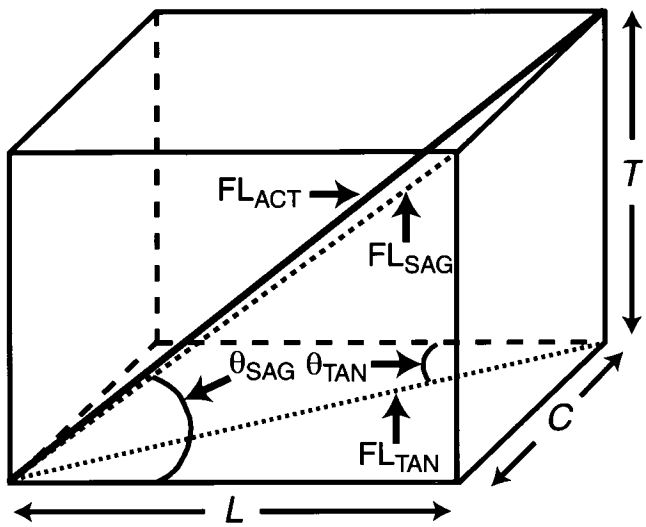

Figure 9. The imaginary polygon used to calculate strain on the model IM-1 and IM-2 collagen fibers during simulated jet locomotion. Only the model IM-1 collagen fiber (solid gray line) is shown. See the Appendix for more detail.

motion, however, result in the compression of IM-2 collagen fibers for a longer portion of the jet cycle (Fig. 8C). Thus, if the mantle of a hatchling stage squid lengthens even a small amount, the IM-2 collagen fibers will store elastic energy only during vigorous jet locomotion.

The young 2 model predicts similar increases in the range of possible changes in mantle circumference with increases in mantle length during jetting (Fig. 8D). In contrast to the hatchling stage model, the young 2 stage model predicts that only increases in mantle length greater than 10% will result in compression of the IM-2 collagen fiber during jet locomotion (Fig. 8D). Thus, modest increases in mantle length will permit elastic energy storage in IM-2 collagen fibers during low-amplitude movements of the mantle.

Can IM-1 and IM-2 fiber angles predict mantle kinematics?

The models for IM-1 and IM-2 described above both suggest that a much greater range of mantle circumference change is possible during jet locomotion in newly hatched *S. lessoniana* than in older, larger squid. The models predict that mantle circumference changes up to −45% are possible in hatchling stage squid compared with −25% and −30% in young 2 stage squid. The few published accounts of mantle kinematics support these predictions. In *Loligo opalescens* the range of circumference change during vigorous jet locomotion is at least 10% greater in hatchling animals than in older, larger squid (Gilly *et al.*, 1991). Maximum mantle circumference changes are about −40% to −42% in hatchlings and about −30% in mature animals (Gilly *et al.*, 1991). In *Loligo vulgaris*, the maximum mantle circumference changes are about −45% and −30% in hatchling and adult animals, respectively, during escape-jet locomotion (calculated from Packard, 1969). During escape-jet locomotion in *S. lessoniana*, mantle circumference changes −45% and −33% in hatchling stage and young 2 stage squid, respectively (Thompson, 2000; Thompson and Kier, 2001). Even during less vigorous jet locomotion and respiratory mantle movements, the range of mantle circumference change is considerably greater in newly hatched *L. opalescens* (Preuss *et al.*, 1997). Given the assumptions of the geometric models, the measurement errors inherent in the histological methods, the cross-species comparisons, and the lack of consideration for the role of circumferential muscle mechanics in mantle contraction, it is striking that the models accurately predict the maximum amplitude of actual mantle kinematics. Thus, we hypothesize that the arrangement of intramuscular collagen fibers likely plays a crucial role in determining the mechanical properties of squid mantle.

Predictions of elastic energy storage from the IM collagen fiber models

The mathematical models of IM-1 and IM-2 predict ontogenetic changes in the potential of the intramuscular collagen fibers to store elastic energy. During low-amplitude mantle contraction in hatchling stage *S. lessoniana*, the models predict that IM-1 and IM-2 collagen fibers are compressed and, thus, are unable to store elastic energy. This prediction holds if mantle length remains constant during the simulated jet or if mantle length increases (only up to 10% for IM-1 fibers) during the jet. Only during large-amplitude mantle movements (*e.g.*, during vigorous jet locomotion) do the hatchling stage models predict that IM-1 and IM-2 collagen fibers are stretched and, thus, able to store elastic energy. Conversely, the models predict that IM-1 and IM-2 collagen fibers in young 2 stage *S. lessoniana* are stretched as the mantle contracts and, thus, can store elastic energy during jet locomotion.

The hatchling stage models also predict a difference in the relative elongation of IM-1 and IM-2 collagen fibers during jet locomotion. If mantle length remains constant during the jet, a mantle circumference decrease of 18% is required to elongate an IM-1 collagen fiber, whereas a mantle circumference decrease of 33% is necessary to extend an IM-2 collagen fiber. Thus, the hatchling stage models predict that IM-2 collagen fibers may not contribute to elastic energy storage in the mantle except during vigorous jet locomotion.

Volume fraction of collagen

Isolated portions of squid and cuttlefish mantle store elastic energy in experiments that simulate mantle movement during the exhalant phase of jet locomotion (Gosline and Shadwick, 1983a, b; MacGillivray *et al.*, 1999; Curtin *et al.*, 2000). The amount of elastic energy stored in the mantle depends on the volume of collagen in the tissue, the strain experienced by the collagen fibers, and the mechanical properties of the mantle collagen fibers. The volume fraction of collagen in IM-1 and IM-2 increased 68 times and 36 times, respectively, during ontogeny. If IM-1 and IM-2 collagen fibers are strained comparably during locomotion in squid of all ages, and if the mechanical properties of collagen do not change with growth, the elastic energy storage capacity of the mantle is likely to increase dramatically during ontogeny.

Future directions

We have described ontogenetic changes in IM-1 and IM-2 fiber angle and in mantle collagen volume fraction. To analyze these changes further, and to begin testing the predictions of the models, accurate measurement of mantle length during jet locomotion is needed. In addition, the

predictions of the models assume that the mechanical properties of squid mantle collagen do not change during ontogeny. This important assumption needs to be tested, particularly because the mechanical properties of collagen change during the growth of many animals (*e.g.*, Parry and Craig, 1988). Therefore, mechanical tests of intact portions of squid mantle, in combination with data on mantle length during jet locomotion, are necessary to test the predictions of the models and to understand better the ecological and evolutionary implications of ontogenetic changes in the morphology of mantle connective tissue.

Acknowledgments

This research was supported by NSF grants to W.M.K. (IBN-9728707 and IBN-9219495). Grants and fellowships to J.T.T. from the Wilson Fund, the American Malacological Association, and Sigma Xi helped defray research expenses. We thank L. Walsh at the NRCC for her expertise in shipping squid cross-country and E. Burgin for his help in sectioning and staining. We are grateful to the Duke-UNC biomechanics group for discussion of several of the ideas in this paper and to D. Pfennig for statistical advice. Finally, we thank S. A. Wainwright, J. Taylor, and two anonymous reviewers for constructive comments and suggestions on an earlier version of the paper.

Literature Cited

Bone, Q., A. Pulsford, and A. D. Chubb. 1981. Squid mantle muscle. *J. Mar. Biol. Assoc. U.K.* **61:** 327–342.

Cassada, R. C., and R. L. Russell. 1975. The dauerlarva, a post-embryonic developmental variant of the nematode *Caenorhabditis elegans. Dev. Biol.* **46:** 326–342.

Chapman, G. 1958. The hydrostatic skeleton in the invertebrates. *Biol. Rev. Camb. Philos. Soc.* **33:** 338–371.

Clark, R. B. 1964. *Dynamics in Metazoan Evolution.* Clarendon Press, Oxford.

Clark, R. B., and J. B. Cowey. 1958. Factors controlling the change of shape of certain nemertean and turbellarian worms. *J. Exp. Biol.* **35:** 731–748.

Cox, G. N., S. Staprans, and R. S. Edgar. 1981. The cuticle of *Caenorhabditis elegans.* II. Stage-specific changes in ultrastructure and protein composition during postembryonic development. *Dev. Biol.* **86:** 456–470.

Curtin, N. A., R. C. Woledge, and Q. Bone. 2000. Energy storage by passive elastic structures in the mantle of *Sepia officinalis. J. Exp. Biol.* **203:** 869–878.

Gilly, W. F., B. Hopkins, and G. O. Mackie. 1991. Development of giant motor axons and neural control of escape responses in squid embryos and hatchlings. *Biol. Bull.* **180:** 209–220.

Gosline, J. M., and R. E. Shadwick. 1983a. The role of elastic energy storage mechanisms in swimming: an analysis of mantle elasticity in escape jetting in the squid, *Loligo opalescens. Can. J. Zool.* **61:** 1421–1431.

Gosline, J. M., and R. E. Shadwick. 1983b. Molluscan collagen and its mechanical organization in squid mantle. Pp. 371–398 in *The Mollusca. Vol. I: Metabolic Biochemistry and Molecular Biomechanics,* P. W. Hochachka, ed. Academic Press, New York.

Gosline, J. M., J. D. Steeves, A. D. Harman, and M. E. DeMont. 1983. Patterns of circular and radial mantle muscle activity in respiration and jetting of the squid *Loligo opalescens. J. Exp. Biol.* **104:** 97–109.

Harris, J. E., and H. D. Crofton. 1957. Structure and function in the nematodes: Internal pressure and cuticular structure in *Ascaris. J. Exp. Biol.* **34:** 116–130.

Kier, W. M. 1992. Hydrostatic skeletons and muscular hydrostats. Pp. 205–231 in *Biomechanics: Structures and Systems. A Practical Approach,* A. A. Biewener, ed. IRL Press at Oxford University Press, New York.

Kier, W. M., and K. K. Smith. 1985. Tongues, tentacles, and trunks: The biomechanics of movement in muscular hydrostats. *Zool. J. Linn. Soc.* **83:** 307–324.

Koehl, M. A. R. 1977. Mechanical diversity of connective tissue of the body wall of sea anemones. *J. Exp. Biol.* **69:** 107–125.

Lee, P. G., P. E. Turk, W. T. Yang, and R. T. Hanlon. 1994. Biological characteristics and biomedical applications of the squid *Sepioteuthis lessoniana* cultured through multiple generations. *Biol. Bull.* **186:** 328–341.

López-DeLeón, A., and M. Rojkind. 1985. A simple micromethod for collagen and total protein determination in formalin-fixed paraffin-embedded sections. *J. Histochem. Cytochem.* **33(8):** 737–743.

MacGillivray, P. S., E. J. Anderson, G. M. Wright, and M. E. DeMont. 1999. Structure and mechanics of the squid mantle. *J. Exp. Biol.* **202:** 683–695.

Messenger, J. B., M. Nixon, and K. P. Ryan. 1985. Magnesium chloride as an anaesthetic for cephalopods. *Comp. Biochem. Physiol.* **82C:** 203–205.

Moltschaniwskyj, N. A. 1994. Muscle tissue growth and muscle fibre dynamics in the tropical loliginid squid *Photololigo* sp. (Cephalopoda: Loliginidae). *Can. J. Fish. Aquat. Sci.* **51:** 830–835.

Mommsen, T. P., J. Ballantyne, D. MacDonald, J. Gosline, and P. W. Hochachka. 1981. Analogues of red and white muscle in squid mantle. *Proc. Nat. Acad. Sci. USA* **78(5):** 3274–3278.

Montes, G. S., and Junqueira, L. C. U. 1988. Histochemical localization of collagen and of proteoglycans in tissues. Pp. 41–72 in *Collagen. Vol. II. Biochemistry and Biomechanics,* M. E. Nimni, ed. CRC Press, Boca Raton, FL.

Packard, A. 1969. Jet propulsion and the giant fibre response of *Loligo. Nature* **221:** 875–877.

Packard, A., and E. R. Trueman. 1974. Muscular activity of the mantle of *Sepia* and *Loligo* (Cephalopoda) during respiratory movements and jetting, and its physiological interpretation. *J. Exp. Biol.* **61:** 411–419.

Parry, D. A. D., and A. S. Craig. 1988. Collagen fibrils during development and maturation and their contribution to the mechanical attributes of connective tissue. Pp. 1–23 in *Collagen. Vol. II: Biochemistry and Biomechanics,* M. E. Nimni, ed. CRC Press, Boca Raton, FL.

Preuss, T., Z. N. Lebaric, and W. F. Gilly. 1997. Post-hatching development of circular mantle muscles in the squid *Loligo opalescens. Biol. Bull.* **192:** 375–387.

Segawa, S. 1987. Life history of the oval squid, *Sepioteuthis lessoniana* in Kominato and adjacent waters central Honshu, Japan. *J. Tokyo Univ. Fish.* **74(2):** 67–105.

Shadwick, R. E., and J. M. Gosline. 1985. The role of collagen in the mechanical design of squid mantle. Pp. 299–304 in *Biology of Invertebrate and Lower Vertebrate Collagens,* A. Bairati and R. Garrone, eds. Plenum Press, New York.

Sweat, F., H. Puchtler, and S. I. Rosenthal. 1964. Sirius red F3BA as a stain for connective tissue. *Arch. Pathol.* **78:** 69–72.

Thompson, J. T. 2000. The ontogeny of mantle structure and function in the oval squid, *Sepioteuthis lessoniana* (Cephalopoda: Loliginidae). Ph.D. dissertation, University of North Carolina at Chapel Hill.

Thompson, J. T., and W. M. Kier. 2001. Ontogenetic changes in mantle kinematics during escape-jet locomotion in the oval squid, *Sepioteuthis lessoniana* Lesson, 1830. *Biol. Bull.* **201:** 154–166.

Wainwright, S. A. 1970. Design in hydraulic organisms. *Naturwissenschaften* **57:** 321–326.

Wainwright, S. A., and M. A. R. Koehl. 1976. The nature of flow and the reaction of benthic cnidaria to it. Pp. 5–21 in *Coelenterate Ecology and Behavior,* G. O. Mackie, ed. Plenum Press, New York.

Wainwright, S. A., W. D. Biggs, J. D. Currey, and J. M. Gosline. 1976. *Mechanical Design in Organisms.* Princeton University Press, Princeton.

Ward, D. V. 1972. Locomotory function of the squid mantle. *J. Zool. (Lond)* **167:** 487–499.

Ward, D. V., and S. A. Wainwright. 1972. Locomotory aspects of squid mantle structure. *J. Zool. (Lond)* **167:** 437–449.

Weibel, E. R. 1979. *Stereological Methods. Vol. 1: Practical Methods for Biological Morphometry.* Academic Press, New York.

Young, J. Z. 1938. The functioning of the giant nerve fibres of the squid. *J. Exp. Biol.* **15:** 170–185.

Zar, J. H. 1996. *Biostatistical Analysis.* Prentice Hall, Upper Saddle River, NJ.

Appendix

The following is a brief summary of the variables, assumptions, and steps used in the calculation of strain on the IM-1 model collagen fiber. The procedure for calculating strain on the model IM-2 collagen fiber is similar to that outlined below and is not shown. The only difference between the two calculations is that the model IM-2 collagen fiber is restricted to plane *CT* (Fig. 1). That simplifies the calculation, in that the IM-2 projected fiber length is the same as the actual fiber length.

Variables (see Fig. 9 in text)

θ_{SAG} = IM-1_{SAG} fiber angle
θ_{TAN} = IM-1_{TAN} fiber angle
L = Polygon length (parallel to mantle length)
C = Polygon width (parallel to mantle circumference)
T = Polygon thickness (parallel to mantle wall thickness)
FL_{SAG} = Projected fiber length of the IM-1 collagen fiber in the sagittal plane
FL_{TAN} = Projected fiber length of the IM-1 collagen fiber in the tangential plane
FL_{ACT} = Actual length of IM-1 collagen fiber

Initial conditions

$\theta_{SAG\ Hatch} = 32°$ $\theta_{SAG\ Young2} = 43°$
$\theta_{TAN\ Hatch} = 39°$ $\theta_{TAN\ Young2} = 32°$
$FL_{SAG} = 1.0$ (arbitrary units)
$L = FL_{SAG} \cos \theta_{SAG}$
$T = FL_{SAG} \sin \theta_{SAG}$

Steps

(1). Calculate polygon width, C:
$$C = L \tan \theta_{TAN}$$

(2). Calculate polygon volume:
$$\text{Volume} = LTC$$
Note, the volume of the model polygon was assumed to remain constant during the simulation.

(3). Keeping volume constant, vary side C (from $1.0C$ to $0.5C$) to mimic circumferential muscle contraction during jet locomotion. Solve for polygon thickness, T:
$$T = \text{Volume} \div LC$$
Note, for the calculations in which mantle length was constant, side L was held constant as side C was varied. For the calculations in which mantle length was allowed to increase, side L was increased 5%, 10%, or 15% in length as side C was varied.

(4). Calculate the projected fiber length of the IM-1_{TAN} collagen fiber, FL_{TAN}:
$$FL_{TAN} = \sqrt{(C^2 + L^2)}$$

(5). Calculate the actual length of the IM-1 collagen fiber, FL_{ACT}:
$$FL_{ACT} = \sqrt{(T^2 + FL_{TAN}^2)}$$

(6). Calculate θ_{SAG} and θ_{TAN}:
$$\tan \theta_{SAG} = T \div L$$
$$\tan \theta_{TAN} = C \div L$$